Angewandte Chemie
Eine Zeitschrift der Gesellschaft Deutscher Chemiker

Supporting Information

69451 Weinheim, Germany

Flexible, Light-Weight, Ultrastrong, and Semiconductive Carbon Nanotube Fibers for a Highly Efficient Solar Cell**

Tao Chen, Shutao Wang, Zhibin Yang, Quanyou Feng, Xuemei Sun, Li Li, Zhong-Sheng Wang, and Huisheng Peng**

anie_201003870_sm_miscellaneous_information.pdf

Supporting Information

Experimental Section

Nanotubes were synthesized by a typical chemical vapor deposition in a quartz tube furnace using catalyst of Fe(1nm)/Al_2O_3(10nm) on silicon wafer. The synthetic details of nanotubes as well as their assembly into fibers had been reported elsewhere[9]. The rotation speeds of the microprobe typically ranged from 1000 to 3000 rad/min during the fiber spinning. In order to fabricate high-quality devices, the as-spun nanotube fibers were first transferred onto the FTO conductive glass (F–doped SnO_2, 15 ohm/square, transmittance 90%, Nippon Sheet Glass Co., Japan) or the flexible ITO (indium tin oxide) coated on PEN substrate (12 ohm/square, Peccell Co., Japan), and wetted by dropping ethanol onto the sample for better contact between the nanotube fibers and the conductive FTO substrates. Then, the nanotube fibers on the FTO conductive glass were heated in the muffle furnace at 350 ^oC (or at 130 ^oC for the ITO–PEN substrates) for about 0.5h. Here the nanotube fibers were stabilized on the electrode through van der Waals force after the above treatments. After the temperature was decreased to and kept at about 120 ^oC, the activated nanotube fibers on the conductive substrates were immersed into the solution of N719 (0.3 mM in CH_3CN) for about 12h. Finally, the nanotube fibers on the substrate were washed using dry ethanol to rinse away dyes adsorbing on the substrates. The Pt-coated FTO conductive glass or ITO–PEN with two holes was used as counter electrode. The working electrode and the counter electrode with a Surlyn frame as spacer were sealed by pressing them together at a pressure of about 200 psi and a temperature of 100 ^oC. Then, the redox electrolyte, which consists of 0.1 M LiI, 0.05 M I_2, 0.6 M dimethyl-3-n-propyl-imidazolium iodide and 0.5 M 4-tert butyl-pyridine in dehydrated acetonitrile, was introduced into the cell through the two holes on the back of the counter electrode. Finally, the holes were sealed by covering a Surlyn sheet and a piece of microscope objective glass, which was pressed at 100 ^oC. Some

more information about the device structure and measurement has been provided in Figures S7 and S8.

The structure of nanotubes was characterized by transmission electron microscopy (TEM, JEOL JEM-2100F operated at 200 kV), and the structure of nanotube fibers was analyzed by scanning electron microscopy (SEM, Hitachi FE-SEM S-4800 operated at 1 kV). SEM samples were coated with a thin layer of carbon to improve the resolution before observations. TEM samples were prepared by dropcasting nanotube/ethanol solutions onto copper grids in the open air. Mechanical tests were performed by a Shimadzu Table-Top Universal Testing Instrument. The used fiber was mounted on a paper tab with gauge length of 5 mm, and the fiber diameter was measured by SEM. Confocal laser scanning microscopy was performed at Olympus FV300 with excitation wavelength of 488 nm. Raman measurements were performed on Renishaw inVia Reflex with excitation wavelength of 514.5 nm and laser power of 20 mW at room temperature. UV-vis spectrometer was recorded on Shimadz UV-3150.

The fiber solar cells were measured by recording *J-V* curves with a Keithley 2400 Source Meter under illumination (100 mW/cm^2) of simulated AM1.5G solar light coming from a solar simulator (Oriel-91193 equipped with a 1000 W Xe lamp and an AM1.5 filter). The light intensity was calibrated using a reference Si solar cell (Oriel-91150). IPCE action spectra were measured with an Oriel-74125 system (Oriel Instruments, USA), where intensity of monochromatic light was measured with a Si diode detector (Oriel-71640). The stray light was shielded by a mask with an aperture which is a little larger than the nanotube fiber in size.

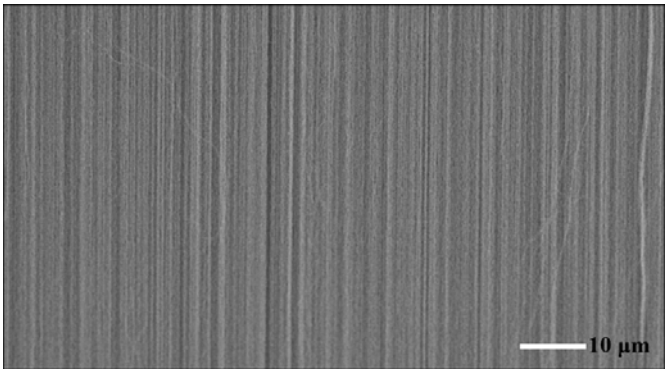

Figure S1. Scanning electron microscopy (SEM) image of a carbon nanotube array taken from the side.

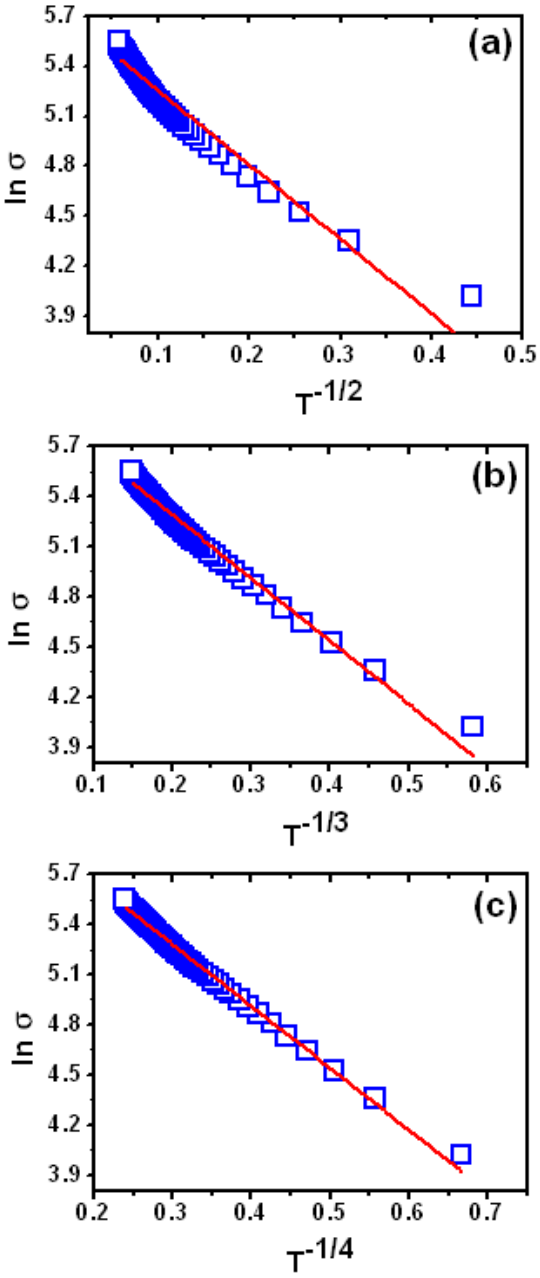

Figure S2. The plots of lnσ *vs.* $T^{-1/(d+1)}$ based on the Mott's variable range hopping model, where σ is the electrical conductivity, T is the temperature, and d is the dimensionality. For these plots, (a) one-dimensional hopping mechanism, i.e., d = 1; (b) two-dimensional hopping mechanism, i.e., d = 2; (c) three-dimensional hopping mechanism, i.e., d = 3.

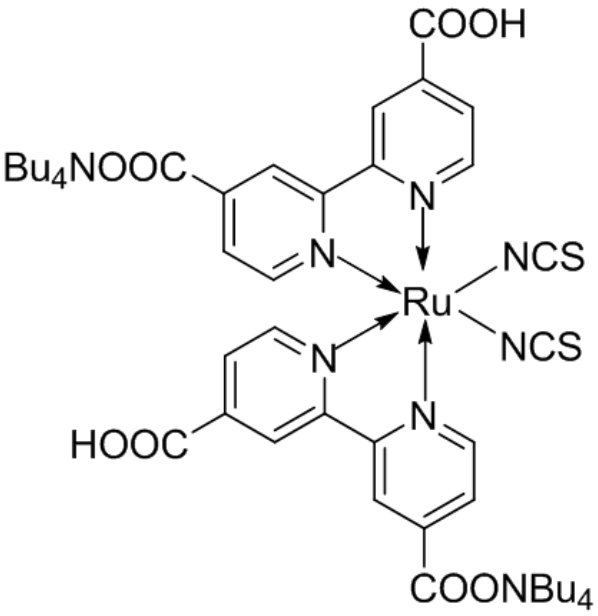

Figure S3. Chemical structure of N719.

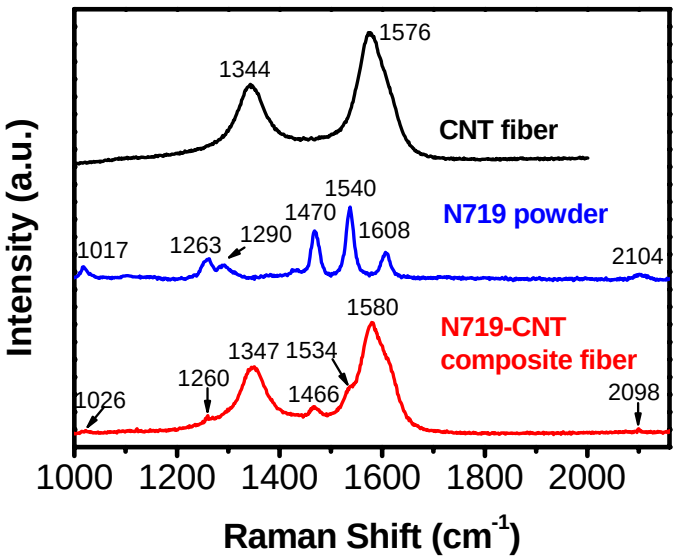

Figure S4. Raman spectra of pure nanotube fiber (black line), pure N719 (blue line), and nanotube/N719 composite fiber (red line).

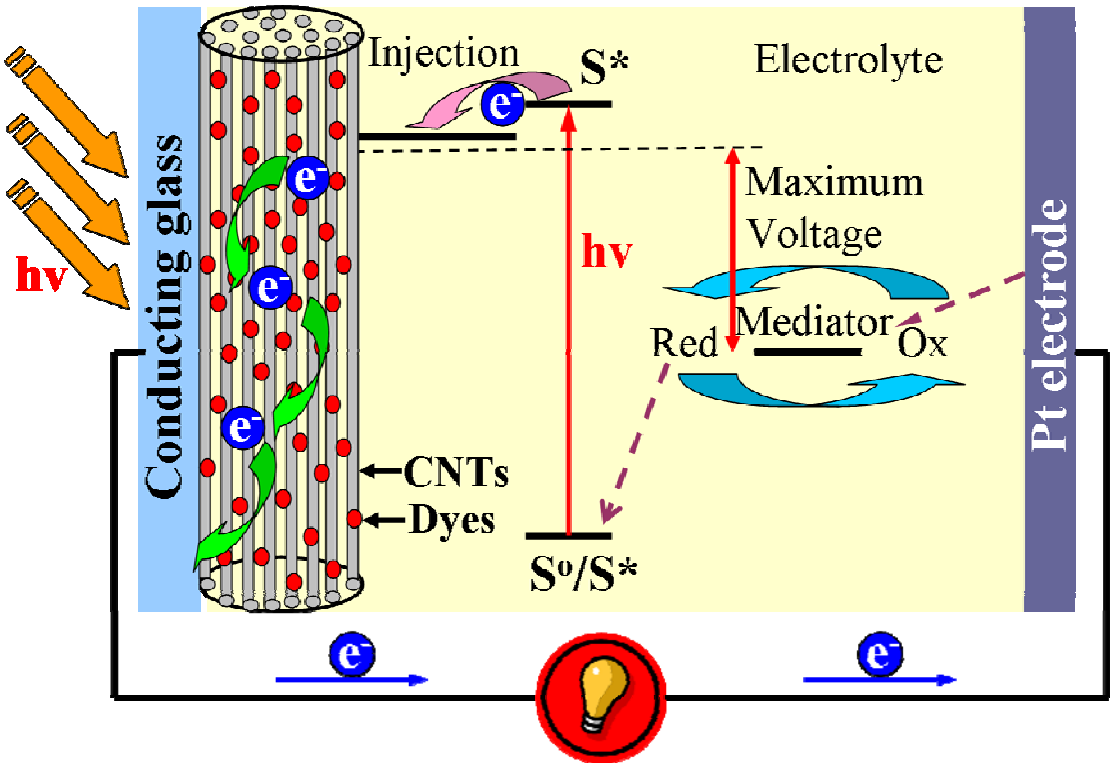

Figure S5. Schematic diagram of the production and transportation of photoelectron in a nanotube fiber solar cell. CNTs represents carbon nanotubes.

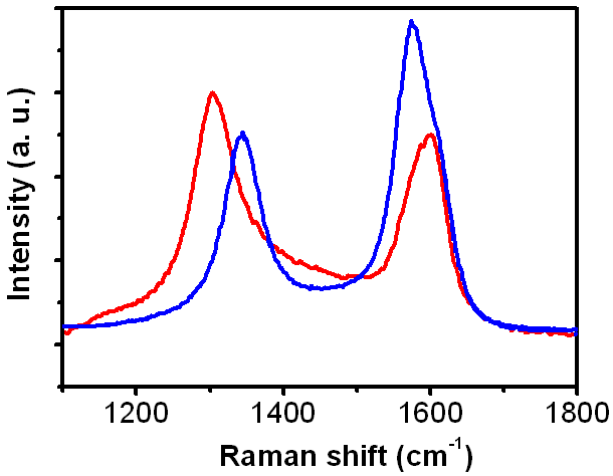

Figure S6. Raman spectra of nanotube fibers before (blue line) and after acidic treatment (red line).

Table S1. Performance parameters of the novel solar cells based on the nanotube fibers with different diameters.

Diameter (μm)	Jsc (mA/cm^2)	Voc (V)	FF	η (%)
6	11.0±0.7	0.45±0.02	0.41±0.03	2.03±0.20
10	7.6±0.2	0.48±0.03	0.39±0.01	1.42±0.10
13	3.1±0.3	0.25±0.04	0.40±0.02	0.31±0.03
17	2.1±0.1	0.18±0.01	0.38±0.02	0.14±0.02

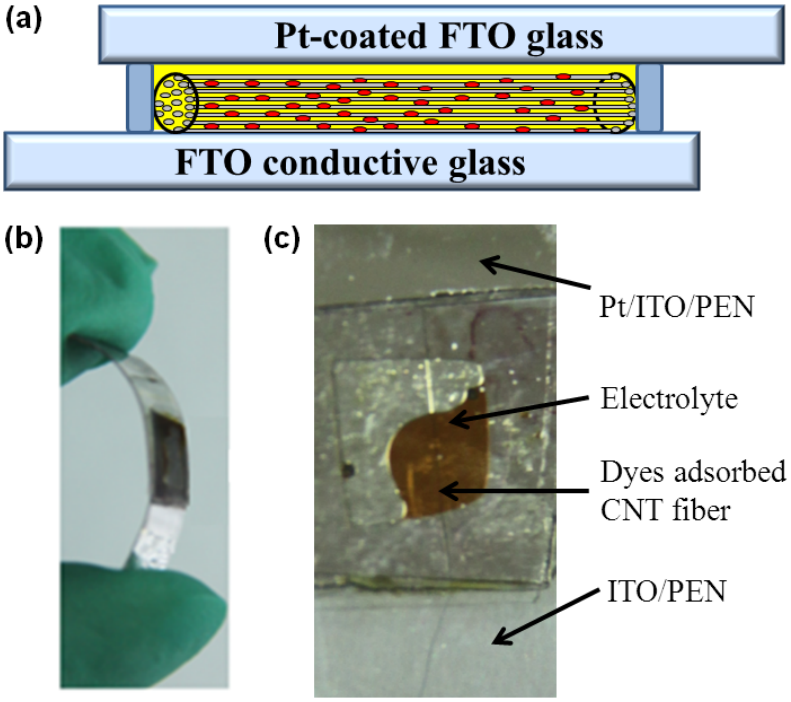

Figure S7. The novel solar cells based on the nanotube fibers. (a) The scheme showing the device structure (yellow for electrolyte, red for dye, and gray cylinder for nanotubes). (b) and (c) Photographs of representative devices.

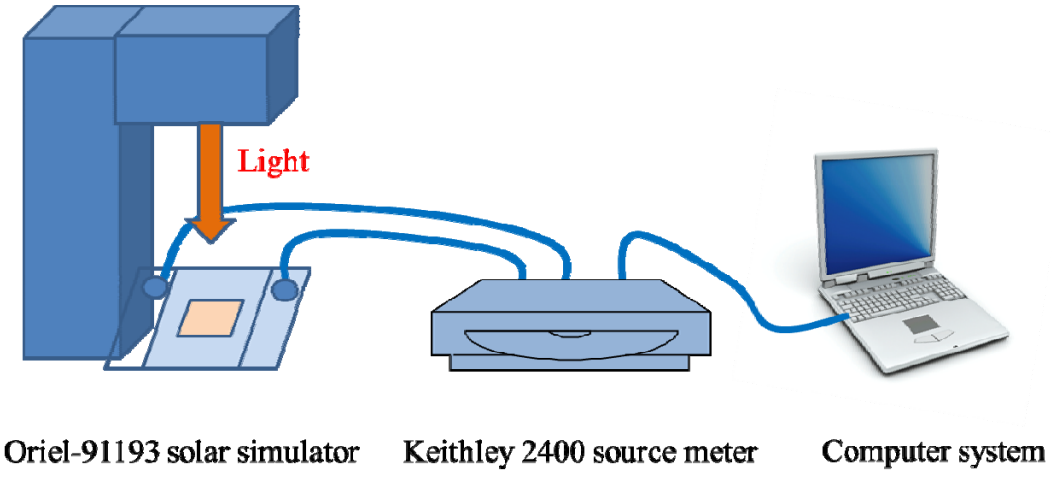

Figure S8. The setup scheme for obtaining the J–V curves of the devices.